Silicon nanoparticle-ZnS nanophosphors for ultraviolet-based white light emitting diode

Matthew Stupca, Osama M. Nayfeh, Tuan Hoang, Munir H. Nayfeh, Bahjat Alhreish et al.

Related Articles

Ultrabroadband terahertz conductivity of Si nanocrystal films
Appl. Phys. Lett. 101, 211107 (2012)

Spectral patterns underlying polarization-enhanced diffractive interference are distinguishable by complex trigonometry
Appl. Phys. Lett. 101, 183104 (2012)

Near-infrared enhanced carbon nanodots by thermally assisted growth
Appl. Phys. Lett. 101, 163107 (2012)

Nanocluster Si sensitized Er luminescence: Excitation mechanisms and critical factors for population inversion
Appl. Phys. Lett. 101, 141907 (2012)

High energy-resolution electron energy-loss spectroscopy study on the near-infrared scattering mechanism of $Cs_{0.33}WO_3$ crystals and nanoparticles
J. Appl. Phys. 112, 074308 (2012)

Additional information on J. Appl. Phys.

Journal Homepage: http://jap.aip.org/

Journal Information: http://jap.aip.org/about/about_the_journal

Top downloads: http://jap.aip.org/features/most_downloaded

Information for Authors: http://jap.aip.org/authors

Silicon nanoparticle-ZnS nanophosphors for ultraviolet-based white light emitting diode

Matthew Stupca,[1] Osama M. Nayfeh,[1] Tuan Hoang,[1] Munir H. Nayfeh,[1,a)] Bahjat Alhreish,[2] Jack Boparai,[2] Abdullah AlDwayyan,[3] and Mohamad AlSalhi[3]
[1]*Department of Physics, University of Illinois at Urbana-Champaign, 1110 W. Green Street, Urbana, Illinois 61801, USA*
[2]*Nanosi Advanced Technologies, 2111 S. Oak Street, Champaign, Illinois 61820, USA*
[3]*Physics and Astronomy Department, King Saud University, P.O. Box 2455, Riyadh 11451, Saudi Arabia*

Present red phosphor converters provide spectra dominated by sharp lines and suffer from availability and stability issues which are not ideal for color mixing in display or solid state lighting applications. We examine the use of mono dispersed 3 nm silicon nanoparticles, with inhomogeneously broadened red luminescence as an effective substitute for red phosphors. We tested a 3-phase hybrid nanophosphor consisting of ZnS:Ag, ZnS:Cu,Au,Al, and nanoparticles. Correlated color temperature is examined under UV and LED pumping in the range 254, 365–400 nm. The temperature is found reasonably flat for the longer wavelengths and drops for the shorter wavelengths while the color rendering index increases. The photo stability of the phosphors relative to the silicon nanoparticles is recorded. The variation in the temperature is analyzed in terms of the strength of inter-band–gap transition and continuum band to band transitions. © *2012 American Institute of Physics*. [http://dx.doi.org/10.1063/1.4754449]

INTRODUCTION

Recently, attention turned to the development of solid state white lighting in which the output of three wide band phosphor converters in the blue, green, and red, which are pumped by single UV LED are mixed to produce white light. This is in contrast to blue LED-pumped systems. In those, no blue phosphor component is used and the blue component of the white light is derived from the pumping LED. This posed a fundamental limit to reach high correlated color temperature (CCT) and color rendering index (CRI) at the same time. The interest in the UV-solid state lighting stems from potential to alleviate these problems and enable better color mixing and control, as well as production of stronger white sources that handle bigger areas. In addition, UV LED suffers less blue shift at high driving current condition, hence reducing the color shift between bare LED die and the encapsulated die.

To realize UV-based lighting requires, however, the development of higher power UV LEDs,[1] safe configurations, as well as efficient wide band red converters.[2–14] Few good efficient red phosphors, whether sulfide-, nitride-, or oxide-based have been known. Moreover, their spectra are dominated by sharp line spectra with branching ratios that depend on the UV wavelength, not ideal for color mixing. The red phosphor yttrium oxide-sulfide activated with europium (Y2O2S:Eu), for example, has been investigated in UV-based lighting. Co-doped phosphate materials were recently synthesized for near UV pumping, which provided a peak wavelength of 610 nm.[15] It has been conjectured that the phosphate material might contribute to a white-light source with a luminous efficiency of 45 lm/W and color rendering index greater than 90 at a color temperature of 5600 K. Also,

multi-layered red, green, and blue phosphors showed high CRI of over 90.[16] Recently, (CdSe)ZnSe core–shell QDs nanoparticles as red phosphor were examined for near UV pumping.[17] Despite the fact that the luminescence for a given size of the nanoparticle is sharp due to the direct bandgap, the use of an appropriate size distribution allows the realization of a homogeneously broadened emission band. In this paper, we use Si nanoparticles,[18,19] for which luminescence for a given size is wide as a red band converter for UV-based white solid state LED.

In this paper, we tested a mixture consisting of ZnS:Ag and ZnS:Cu,Au,Al[20,21] for blue and green conversion, respectively, while mono dispersed Si nanoparticles act as the red phosphor. The nano-phosphor mixed in room temperature volcanic silicone (RTV) is examined for excitation in the UV. With the wide emission profiles of the components, the fluorescence of this nano-phosphor composite material easily spans the entire visible range, with full color coverage. CCT temperature and the CRI index with excitation wavelength are examined and analyzed in terms of the strength of inter-band–gap transition and continuum band to band transitions.

EXPERIMENTAL

Si nanoparticles are produced by chemical etching of boron-doped 100 Si wafers.[18,19] We treat the wafer in a mixture of HF and Auric (HAuCl4) acid and hexachloroplatinic (H2PtCl6 · H2O) acid to deposit a platinum catalyst. It is then etched using HF/H2O2/ methanol mixture, followed by sonication in a liquid of choice. When examined the solution is found to be brightly red-orange luminescent under 365 nm irradiation with band head at ∼610 nm. The phosphors we used are commercial grade. Colloids of ZnS:Ag and
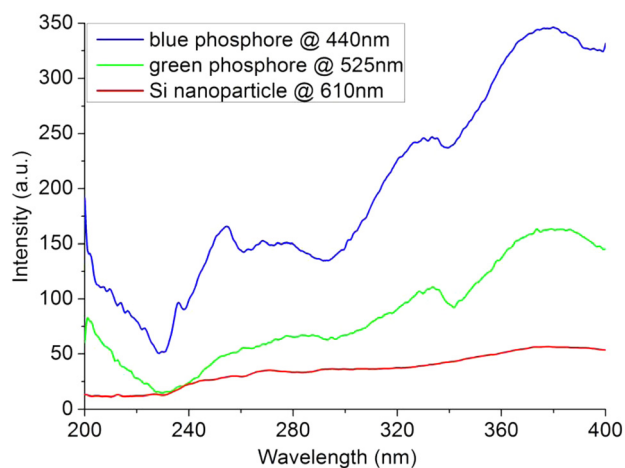
a)m-nayfeh@illinois.edu.

FIG. 1. Excitation spectra of thin films the three components: blue phosphor (blue curve) (top), green phosphor (green curve) (middle), and red silicon nanoparticles (red curve) (bottom) when each is monitored at its maximum response at 440, 525, and 610 nm, respectively. The film thickness and area are arbitrary. The relative signal size is not indicative of the relative efficiency.

ZnS:Cu,Au,Al are luminescent under excitation with 365 nm with band heads at 440 and 525 nm, respectively. Figure 1 gives the excitation spectra of thin films of arbitrary thickness and area of the three components blue and green phosphors and red Si nanoparticles when each is monitored at its maximum response at 440, 525, and 610 nm, respectively. The relative signal size is not indicative of the relative efficiency. The figure shows that when the wavelength of excitation at 365 nm is changed to 254 nm, the efficiency of the blue phosphor and the nanoparticles each drop to the 50% level, whereas the green phosphor efficiency drops more strongly to the 30% level. Figure 2 (top) and Figure 2 (middle) gives scanning electron microscopy (SEM) images of the blue and green phosphors placed on single crystal silicon substrate. Figure 2 (bottom) gives a transmission electron microscopy (TEM) image of the silicon nanoparticles placed on a graphite grid.[22,23] The Si particles stay suspended in the colloid. The phosphors tend to quickly precipitate, however. To avoid precipitation during the curing of the RTV, we premixed the RTV components and allowed the mixture to become viscous enough to achieve stable dispersions. The components are not layered; rather they are mixed thoroughly to achieve a homogeneous mixture. Although the red luminescent nanoparticles absorb at the onset of their quantum confinement band gap of 2.2 eV, i.e., in the red wing of the green of the phosphor, their strongest absorption is in the UV/blue. The CCT temperature of the white light is obtained from the spectral power density (SPD) and the standard observer's color matching functions (CMFs), and the CIE 1960 UCS Planckian locus. The CRI index is calculated and compared to that of the standard illuminant D65. The samples were examined under excitation from a near UV-blue LED at 390 nm, and 365 nm and 254 nm from a mercury lamp.

RESULTS AND ANALYSIS

Figure 3 (top) gives normalized spectra taken under 365 nm of ZnS:Ag, ZnS:Cu,Au,Al and red nanoparticles indi-
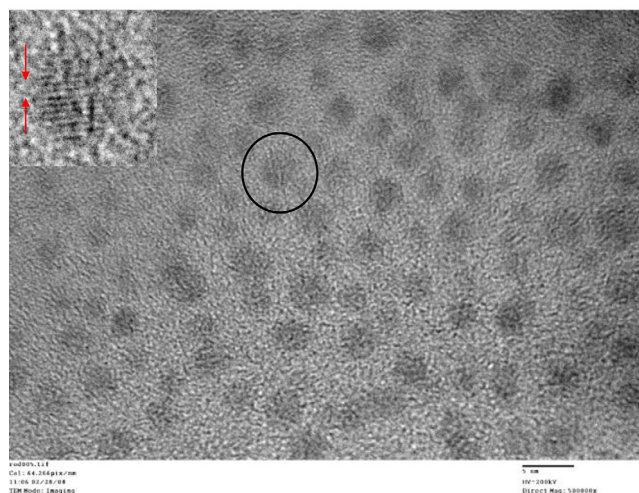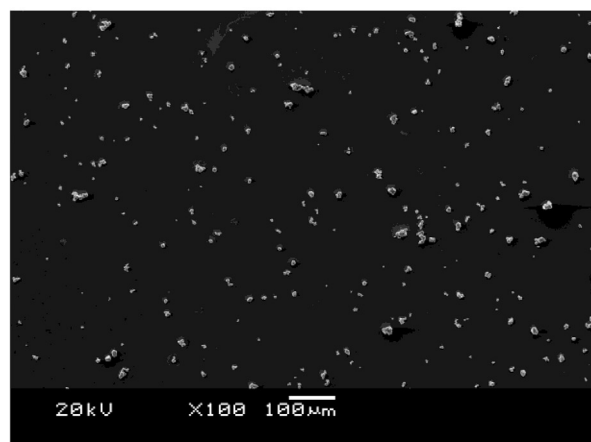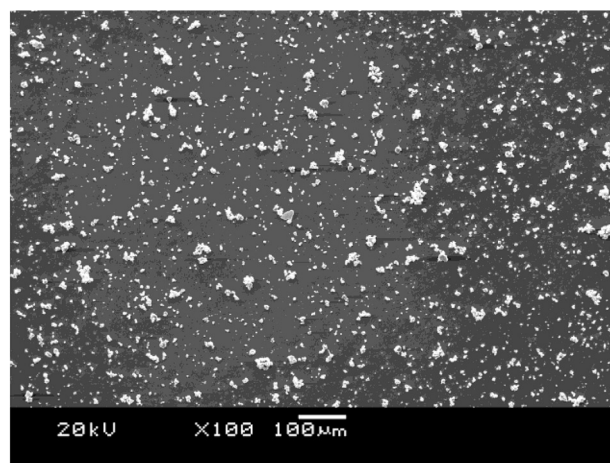

FIG. 2. SEM images of the blue (top) and green phosphors (middle) placed on single crystal silicon substrate. TEM image of the silicon nanoparticles (bottom) placed on a graphite grid.

vidually dispersed in RTV providing blue (410–550 nm), green (470–600 nm), and red (550–800 nm) bands, respectively. The figure gives also the normalized spectrum of a mixture of the three components. The nanophosphor mixture shows a broad spectrum covering the entire range of the visible from 400 to 800 nm. For reference, we give in the figure the normalized spectrum of pure RTV; it is observed to be weakly fluorescent in the blue part of the spectrum in the range 420–550 nm. Figure 3 (bottom) presents the corresponding luminescent
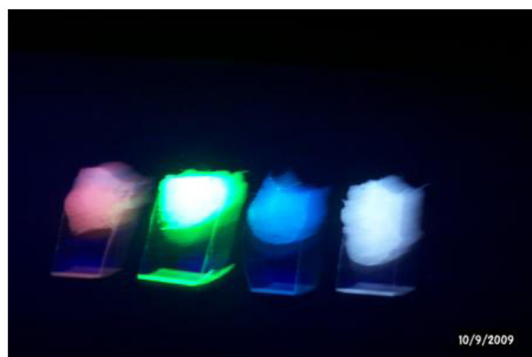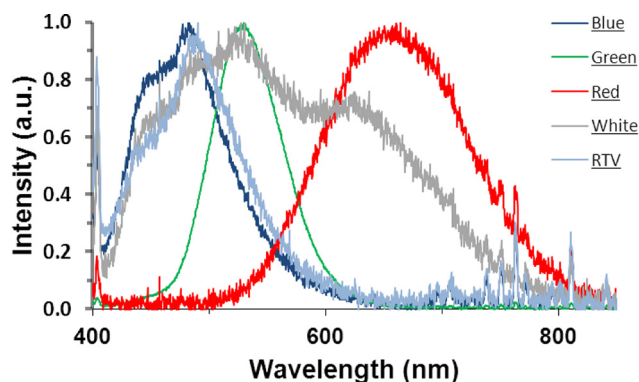
FIG. 3. (Top) Normalized emission spectra of ZnS:Ag (blue), ZnS:Cu,Au,Al (green) and Si nanoparticles (red) individually dispersed in RTV under the excitation of 365 nm radiation. The gray spectrum is due to a mixture of the three components dispersed in RTV under excitation of 365 nm. For reference, we give in the figure the normalized spectrum of pure RTV (light blue). (Bottom) (left to right) the corresponding luminescent images of the individual components and of the mixture under excitation of 365 nm radiation

images of the individual components and of the mixture. The luminescence from the RTV-nanophosphor mixture is bright white. When the individual components or mixture are inspected, emission is found to be isotropic indicating homogeneous mixing with no segregation. Starting from components of the blue and green phosphors and nanoparticle with unknown concentrations but recorded optical response, required volumes were chosen iteratively to arrive at certain color mixtures as shown in Figure 4, which gives spectra of three samples of different composition ratios giving white light. This procedure is found to be reasonably effective to optimize ratios to match required CCT and CRI values. We examined white samples with excitation using commercial UV LEDs at 390 nm and 365 nm, whose spectra are shown in Figure 5. Figure 5 gives also spectra of two white samples using the commercial UV LED at 390 nm. The 390 nm LED may have a small tail background in the blue as shown in the magnified solid version in Figure 5.

The CCT temperature of the white samples is obtained from the SPD using three standard known steps. We first calculated the inner product of the SPD with the standard observer's CMFs. The fitting of the CIE standard observer's color matching function was done on Figure 4 (top) using the interpolation. This yielded the tristimulus values $(X, Y, Z) = (80.0, 100.0, 104.9)$ (after normalizing for $Y = 100$). Using these values, we calculated the xy chromaticity values to be
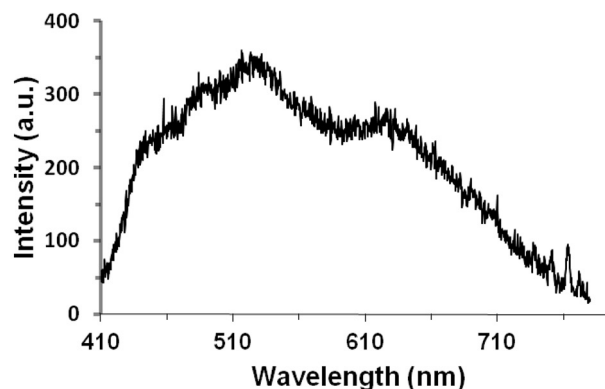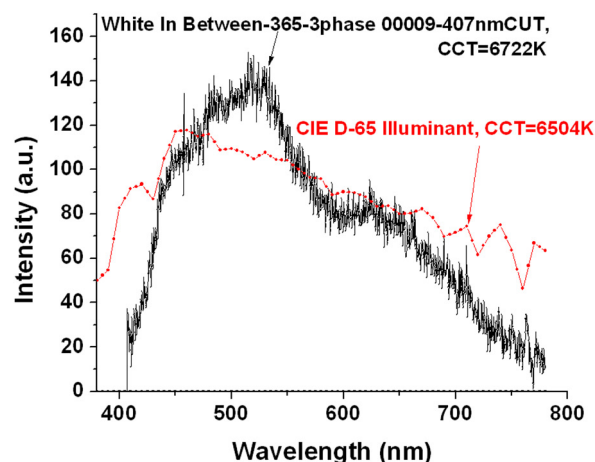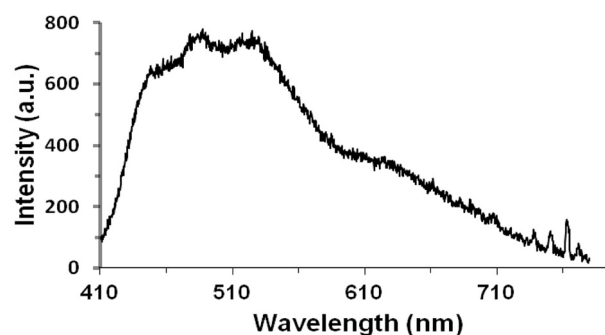

FIG. 4. Luminescence spectra of three shades of white light using different branching ratios of the blue and green phosphors and red Si nanoparticles. The spectra were analyzed for CCT (top) 7981 K; (middle) 6722 K; and (bottom) 5560 K. In (middle), we also present the spectrum of the CIE standard illuminant D65 standard of solar radiation.

$x = 0.2809$, $y = 0.3510$. We converted these chromaticities to the CIE 1960 UCS *u and v coordinates*: $u = 0.1690$, $v = 0.3167$, which according to CIE 1960 UCS gives 7981 K on the Planckian locus, which has a co-ordinate of (0.2809, 0.3510). This temperature is far from 6504 K, which is the CCT of D-65 illuminant, the CIE standard for daylight. Similar calculations gave CCTs of 6722 K and 5560 K for the two other spectra of Figure 4 (middle-bottom).

To control and optimize the nano composition, one needs to calculate the CRI index relative to that of the solar standard spectrum. In Figure 4 (middle), we also present the
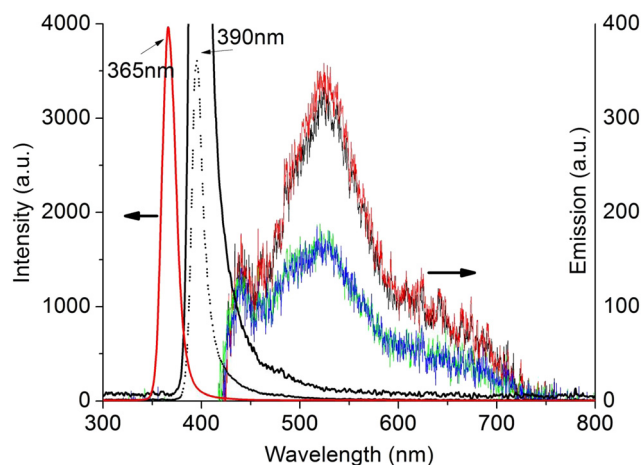
FIG. 5. (Right vertical scale) wideband luminescence spectra of two shades of white light using excitation by a commercial UV LED at 390 nm. (Left vertical scale) the spectral distribution of the 365 nm and the 390 nm UV LED sources used in our studies. The solid spectrum is a magnified version of the 390 nm spectrum (dotted) to display its blue content.
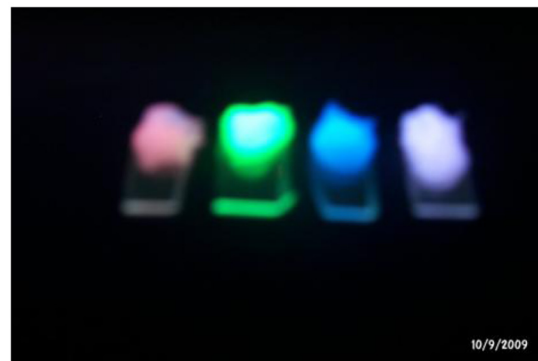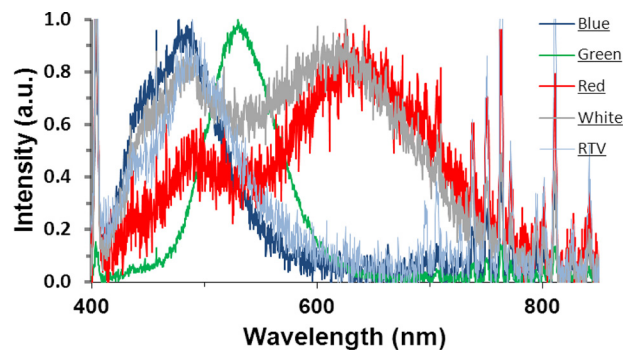

FIG. 6. The corresponding result of Figure 3 under excitation of 254 nm radiation. (Top) Normalized emission spectra of ZnS:Ag (blue), ZnS:Cu,Au,Al (green), and Si nanoparticles (red) individually dispersed in RTV under the excitation of 254 nm radiation. The gray spectrum is due to a mixture of the three components dispersed in RTV under excitation of 254 nm. For reference, we give in the figure the normalized spectrum of pure RTV (light blue). (Bottom) (left to right) the corresponding luminescent images of the individual components and of the mixture under excitation of 254 nm radiation.

spectrum of the CIE standard illuminant D65 standard of solar radiation. It is clear that the phosphor spectrum has more green and less deep red and deep blue. In this case, we get a CRI of 10.2. The spectra in Figure 4 (top) and Figure 4 (bottom) matches the solar standard spectrum better, giving CRI of 30 and 55.

The sample studied in Figure 3 was examined under 254 nm. The spectra and images are shown in Figure 6. The figure shows that the spectral distributions of the individual green and blue components remain the same compared to pumping at 365 nm, but the nanoparticles show an additional week blue-green component resulting from some oxygen termination, which supplements the blue-green phosphor components (Figure 3). The quantum efficiency of the components, however, changes as was seen in the excitation curves in Figure 1. Whereas the efficiencies of the red at 610 nm and blue at 440 nm components dropped in proportion, the green efficiency at 525 nm dropped significantly relative to the drop in the blue and red, Figure 7 shows how the spectra of the samples in Figure 4 (top) and Figure 4 (middle), respectively, transform under excitation at 254 nm. Analysis for the top and bottom spectra gives 7764 K and 4385 K for excitation at 254 nm the CCT compared to 7981 K and 5560 K, respectively, for excitation at 365 nm. The corresponding CRI was calculated to be 83 and 50, respectively, with the improvement attributed to the decrease of the green efficiency. It is clear that one should be able to optimize the ratios of the three components to achieve the required CCT temperature and CRI.

We examined the stability of the CCT temperature under UV radiation. We spin coated phosphors and nanoparticles on a glass substrate. We used a Nichia UV LED at 371 nm. Under LED irradiation, variations are quite slow and weak. To accelerate the study, we used instead the intense continuous wave UV laser beam from a HeCd laser at 330 nm. The 20 mW output is focused to a 3 mm spot at the sample. Figure 8 (top) displays the time development of the spectrum of a mixture of green phosphor and nanopar-

ticles under continuous irradiation. Figure 8 (bottom) gives the time development at the head of the phosphore and nanoparticle bands. Initially, over the first 15 min, the luminescence of both the phosphor and the nanoparticles drop strongly, with the particle luminescence dropping more rapidly than that of the phosphor. Beyond this point, the two become much more stable and track each other quite well. It is feasible to take these transient differences into account when targeting certain CCTs and CRIs. The profile of the drop in the luminescence is not due to the degradation of the RTV matrix as this kind of profile drop has also been observed when nanoparticles are in a colloid of isopropyl alcohol. The phenomenon takes place in fresh samples and the basic mechanism is under investigation.

DISCUSSION

It is interesting to discuss the variation of the white light characteristics as a function of the excitation wavelength. In general, due to the Stoke shift, the energy loss increases as the excitation wavelength decreases. Using shorter wavelength excitation can modulate the CRI and CCT but may cause a decrease in the efficiency at the same times. In principle, the optimization of the phosphor composition would be done at the excitation wavelength of the pumping UV, which is preferably chosen close to the emission wavelength.
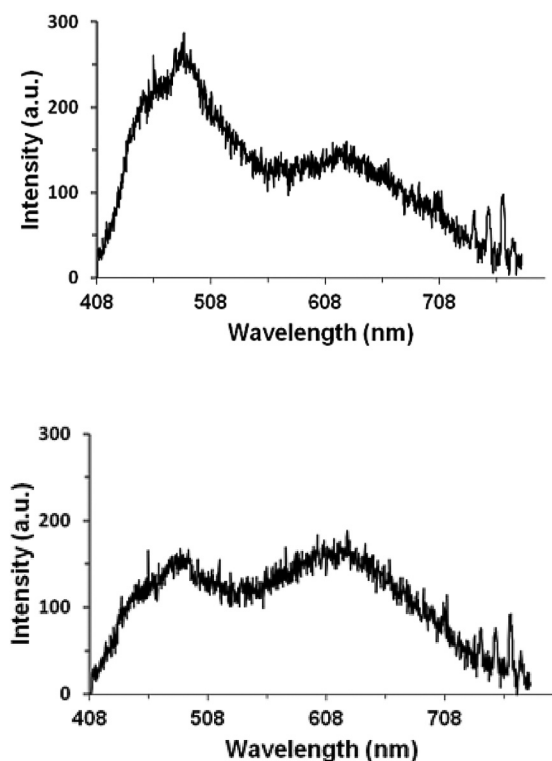
FIG. 7. Spectra of the two shades of white samples given in 4a and 4b under excitation at 254 nm, giving CCT (top) 7764 K and (bottom) 4385 K.

The variation in the color temperature for UV excitation at the shorter 254 nm wavelength observed can be explained in terms of the nature of the states involved.[24,25] In the green phosphor, the host ZnS is prepared under an excess of sulfide ion (S^{2-}) concentration to remove sulfur traps. The state of the dopant Al^{3+} substitutional of Zn (Al_{Zn}) traps electrons from photoexcited electron-hole pairs to form a donor state, which lies below the conduction band edge, and from which emission proceeds. On the other hand the state of the dopant Cu^+ substitutional of Zn^{2+} (Cu_{Zn}) traps holes to form an accepter state that lies above the valence band edge, which constitutes the ground state. Thus, excitation proceeds more efficiently via inter-band-gap states. For the blue phosphor, ZnS is prepared under a deficiency of sulfide ion (S^{2-}) concentration; hence the excited state is a sulfur vacancy state (V_S), which traps electrons to form shallow donor levels just below the conduction band edge. Similar to the green case, Cu^+ substitutionally situated at a Zn^{2+} site (Cu_{Zn}) forms an accepter ground level. Note that V_S lies above Al_{Zn}, much closer to the edge of the conduction band. Thus, in the blue phosphor, excitation proceeds more efficiently via valence band to conduction band transitions of the ZnS host crystal. For the nanoparticle, excitation proceeds more efficiently via valence band to conduction band transitions of Si, followed by electron relaxation and trapping into high quantum efficiency[26] emitting state within the band gap of the particle. Due to the discrete nature of the states, the inter-band–gap transition is sensitive to wavelength, and drops as the photon energy increases in the UV. On the other hand, due to the continuum nature of the band to band transitions, excitation in the blue phosphor and in the particles is less sensitive to wavelength as the photon energy increases. The fact that the
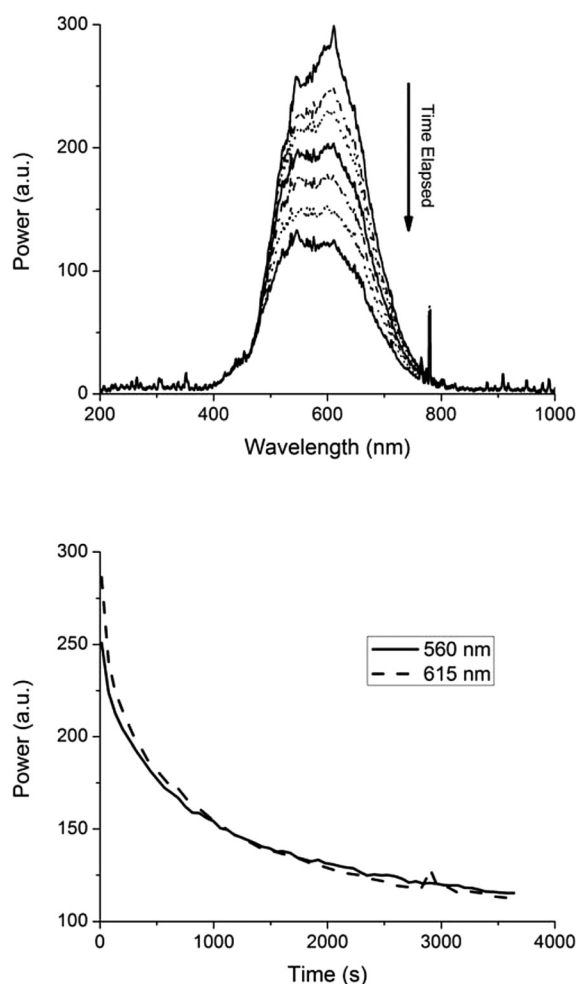

FIG. 8. Time development of the spectrum of a thin film of mixture of green phosphor and red silicon nanoparticles under irradiation by a CW laser beam at 330 nm. (Top) full spectrum. Arrow shows direction of time elapsed. Top spectrum was taken at zero time and the bottom spectrum was taken after 1 h. (bottom) signal at 560 nm (peak of phosphor band) and 610 nm (peak of silicon nanoparticle band).

measured spectral distribution of the blue and red bands stays the same is consistent with this analysis. The variation in the excitation efficiencies with wavelength results in the change of the intensities, hence temperature. The emerging blue-green component in the silicon nanoparticle luminescence makes their spectrum wider, allowing better tuning to the solar spectrum, hence better CRI.

In conclusion, we described a 3-phase nanophosphor for UV-based white solid state LED lighting. We use ZnS:Ag, and ZnS:Cu,Au,Al for blue and green conversion, respectively, and mono dispersed 3 nm Si nano particles as a red phosphor. With wide emission profiles for all components, we can achieve predesigned color characteristics in terms of CCT and CRI simultaneously for excitation in the range 350–400 nm.

ACKNOWLEDGMENTS

[1]T. Nishida, H. Saito, and N. Kobayashi, Appl. Phys. Lett. **79**, 711 (2001); T. Taguchi, IEEJ Trans. Electr. Electron. Eng. **3**, 21 (2008).

[2]T. Kim and S. Kang, J. Lumin. **122–123**, 964 (2007).

[3]J. Jeonga, M. Jayasimhadria, H. S. Leeb, K. Jangb, S. S. Yic, J. H. Jeongd, and C. Kime, Physica B **404**, 2016 (2009).

[4]J. S. Kim, P. E. Jeon, J. C. Choi, H. L. Park, S. I. Mho, and G. C. Kim, Appl. Phys. Lett. **84**, 2931 (2004).

[5]Z. L. Wang, H. B. Liang, J. Wang, M. L. Gong, and Q. Su, Appl. Phys. Lett. **89**, 071921 (2006).

[6]Z. Wu, J. Liu, and M. Gong, Chem. Phys. Lett. **466**, 88 (2008).

[7]R.-J. Xie, N. Hirosaki, and M. Mitomo, J. Electroceram. **21**, 370 (2008).

[8]R.-J. Xie and N. Hirosaki, Sci. Technol. Adv. Mater. **8**, 588 (2007).

[9]D. Jia and D. N. Hunter, J. Appl. Phys. **100**, 113125 (2006).

[10]H. A. Hoppe, H. Lutz, P. Morys, W. Schnick, and A. Seilmeier, J. Phys. Chem. Solids **61**, 2001 (2000).

[11]Y. Q. Li, A. C. A. Delsing, G. de With, and H. T. Hintzen, Chem. Mater. **17**, 3242 (2005).

[12]K. Uheda, N. Hirosaki, Y. Yamamoto, A. Naito, T. Nakajima, and H. Yamamoto, Electrochem. Solid State Lett. **9**, H22 (2006).

[13]R. Le Toquin and A. K. Cheetham, Chem. Phys. Lett. **423**, 352 (2006).

[14]C. Guo, H.-K. Yang, Z. Fu, L. Li, B.-C. Choi, and J.-H. Jeong, J. Am. Ceramic Soc. **92**, 1713 (2009).

[15]J. Cho, H. Kim, C. Sone, Y. Park, Y. S. Kim, S. Kubota, and E. Yoon, Phys. Status Solidi (RRL) **3**, 34 (2009).

[16]T. Fukui, K. Kamon, J. Takeshita, H. Hayashi, T. Miyachi, Y. Uchida, S. Kurai, and T. Taguchi, Jpn. J. Appl. Phys., Part 1 **48**, 112101 (2009).

[17]H. Song and S. Lee, Nanotechnology **18**, 255202 (2007).

[18]G. Belomoin, J. Therrien, A. Smith, S. Rao, S. Chaieb, and M. H. Nayfeh, Appl. Phys. Lett. **80**, 841 (2002).

[19]D. Nielsen, L. Abuhassan, M. Alchihabi, A. Al-Muhanna, J. Host, and M. H. Nayfeh, J. Appl. Phys. **101**, 114302 (2007).

[20]Y. Sato, N. Takahashi, and S. Sato, Jpn. J. Appl. Phys., Part 2 **35**, L838 (1996).

[21]Y. Narukawa, I. Niki, K. Izuno, M. Yamada, Y. Murazaki, and T. Mukai, Jpn. J. Appl. Phys., Part 2 **41**, L371 (2002).

[22]O. M. Nayfeh, D. A. Antoniadis, K. Mantey, and M. H. Nayfeh, Appl. Phys. Lett. **94**, 043112 (2009).

[23]O. Nayfeh, D. Antoniadis, K. Mantey, and M. H. Nayfeh, Appl. Phys. Lett. **90**, 153105 (2007).

[24]K. Manzoor, S. R. Vadera, N. Kumar, and T. R. N. Kutty, Appl. Phys. Lett. **84**, 284 (2004).

[25]K. Manzoor, S. R. Vadera, N. Kumar, and T. R. N. Kutty, Mater. Chem. Phys. **82**, 718 (2003).

[26]A. Smith, Z. Yamani, J. Turner, S. Habbal, S. Granick, and M. H. Nayfeh, Phys. Rev. B **72**, 205307 (2005).